(18) Illers, K. H.; Breuer, H. *J. Colloid Sci.* **1963**, *18*, 1.
(19) Ishida, Y.; Yamafuji, K.; Ito, H.; Takayanagi, M. *Kolloid Z. Z. Polym.* **1962**, *184*, 97.
(20) McCrum, N. G. *J. Polym. Sci.* **1962**, *60*, 53.
(21) Scott, A. H.; Scheiber, D. J.; Curtis, A. J.; Lauritzen, J. I.; Hoffman, J. D. *J. Res. Natl. Bur. Stand., Sect. A* **1962**, *66A*, 269.
(22) Boyd, R. H.; Porter, C. H. *J. Polym. Sci., Part A-2* **1972**, *10*, 647.
(23) Schmieder, K.; Wolf, K. *Kolloid Z.* **1953**, *134*, 149.
(24) Phillips, P. J.; Emerson, F. A.; MacKnight, W. J. *Macromolecules* **1970**, *3*, 771.
(25) Boyd, R. H.; Aylwin, P. A. *Polymer* **1984**, *25*, 330.
(26) Boyd, R. H.; Aylwin, P. A. *Polymer* **1984**, *25*, 340.
(27) Boyd, R. H. *J. Polym. Sci., Polym. Phys. Ed.* **1983**, *21*, 493.
(28) Pechhold, W.; Eisele, U.; Knauss, G. *Kolloid Z. Z. Polym.* **1964**, *196*, 27.
(29) Crissman, J. M.; Passaglia, E. *J. Res. Natl. Bur. Stand., Sect. A* **1966**, *70A*, 225.
(30) Cooper, J. W.; McCrum, N. G. In "Advances in Polymer Science and Engineering"; Pae, K. D., Morrow, D. R., Chen, Y., Ed.; Plenum Press: New York, 1972; p 225.
(31) Illers, K. H. *Kolloid Z. Z. Polym.* **1973**, *251*, 394.
(32) Nakayasu, H.; Markovitz, H.; Plazek, D. J. *Trans. Soc. Rheol.* **1961**, *5*, 261.
(33) McCrum, N. G.; Morris, E. L. *Proc. R. Soc. London, Ser. A* **1966**, *292*, 506.
(34) Porter, C. H.; Boyd, R. H. *Macromolecules* **1971**, *4*, 589.
(35) Boyd, R. H. *J. Chem. Phys.* **1959**, *30*, 1276.
(36) Cole, K. S.; Cole, R. H. *J. Chem. Phys.* **1941**, *9*, 341.
(37) Saito, S. *Kolloid Z. Z. Polym.* **1963**, *189*, 116.
(38) Ferry, J. D. "Viscoelastic Properties of Polymers", 2nd ed.; Wiley: New York, 1970.
(39) Tsai, S. W.; Halpin, J. C.; Pagano, N. J. "Composite Materials Workshop"; Technomic: Stamford, CT, 1968.
(40) Boyd, R. H.; Hasan, A. A. *Polymer* **1984**, *25*, 347.
(41) Yano, S.; Rahalkar, R. R.; Hunter, S. P.; Wang, C. H.; Boyd, R. H. *J. Polym. Sci., Polym. Phys. Ed.* **1976**, *14*, 1877.
(42) Connor, T. M.; Read, B. E.; Williams, G. *J. Appl. Chem.* **1964**, *14*, 74.
(43) Buckley, C. P.; McCrum, N. G. *J. Mater. Sci.* **1973**, *8*, 928.
(44) Davies, G. R.; Owen, A. J.; Ward, I. M.; Gupta, V. B. *J. Macromol. Sci., Phys.* **1972**, *B6*, 215.
(45) Olf, H. G.; Peterlin, A. *J. Polym. Sci., Polym. Phys. Ed.* **1970**, *8*, 753, 771, 791.
(46) Opella, S. J.; Waugh, J. S. *J. Chem. Phys.* **1977**, *66*, 4919.
(47) Hendra, P. J.; Jobic, H. P.; Holland-Moritz, K. *J. Polym. Sci., Polym. Lett. Ed.* **1975**, *13*, 365.
(48) Boyer, R. F.; Snyder, R. G. *J. Polym. Sci., Polym. Lett. Ed.* **1977**, *15*, 315.
(49) Lam, R.; Geil, P. H. *Polym. Bull.* **1978**, *1*, 127; *J. Macromol. Sci., Phys.* **1981**, *B20*, 37.
(50) Jones, J. B.; Barenberg, S.; Geil, P. H. *Polymer* **1979**, *20*, 903.
(51) Cutler, D. J.; Glotin, M.; Hendra, P. J.; Jobic, H.; Holland-Mortiz, K.; Cudby, M. E. A.; Willis, H. A. *J. Polym. Sci., Polym. Phys. Ed.* **1979**, *17*, 907.
(52) Jones, J. B.; Barenberg, S.; Geil, P. H. *J. Macromol. Sci., Phys.* **1978**, *B15*, 329.

Free Volume and the Kinetics of Aging of Polymer Glasses

Richard E. Robertson*

Research Staff, Ford Motor Company, Dearborn, Michigan 48121

Robert Simha[†]

Department of Macromolecular Science, Case Western Reserve University,
Cleveland, Ohio 44106

John G. Curro[‡]

Sandia National Laboratories, Albuquerque, New Mexico 87185. Received July 6, 1983

ABSTRACT: A model for predicting the kinetics of the physical aging of polymer glasses is further developed and is applied to the volume recovery of poly(vinyl acetate). The model is based on the stochastic model previously described by Robertson. It makes use of the free volume or hole fraction arising from the cell model developed by Simha and Somcynsky for equations of state of polymer liquids. The volume recovery predictions computed for poly(vinyl acetate) are compared with the data of Kovacs. Some of the apparent divergence noted by Kovacs between the effective retardation times on approach to equilibrium at a common temperature from different temperatures is explained.

Introduction

Physical aging can affect the properties of plastics and fiber composites years after manufacture. For this reason, many attempts have been made to describe as well as to understand the kinetics of the aging process. Several models exist that can describe many or even most of the characteristics of physical aging. Those most frequently applied to aging problems are related[1] and are the models of Kovacs[2,3] and of Moynihan.[4-6] These models are phenomenological and attempt only to describe formally the kinetics of aging. Two other models attempt to explain the kinetics as well. One if that of Curro, Lagasse, and Simha,[7] which is based on a hole diffusion process. The other is the stochastic model originally suggested by Robertson.[8-11]

In this report, the stochastic model will be explored further. First, we wish to derive the stochastic model for volume relaxation using the free volume suggested by Simha and Somcynsky's cell model for polymer liquids.[12] The free volume suggested by this model is the hole fraction that results from the minimization of the configurational Helmholtz free energy with respect to the hole fraction. The use of this definition of free volume and the resulting temperature coefficient has been shown to yield very satisfactory predictions of the time–temperature shift parameters during the aging of poly(methyl methacrylate) and poly(vinyl acetate) following a downward step in temperature.[13,14] Second, we wish to apply the stochastic model to the volume relaxation of poly(vinyl acetate) and to compare the computed results with the experimental data of Kovacs.[15]

Theory

Equation of State and Free Volume. To model the time-dependent volume contraction and dilatation following changes in temperature, we need the equilibrium volumes at the respective temperatures, the hole fractions or free volumes, and the fluctuations in free volume. These

---

[†] Supported by NSF Grant DMR-80-12232, Polymers Program.
[‡] Supported by U.S. DOE DE-AC04-76 DP00789.

0024-9297/84/2217-0911$01.50/0 © 1984 American Chemical Society

are readily obtained from the cell model developed by Simha and Somcynsky[12] for the equation of state of polymer liquids. For N s-mer molecules occupying the fraction y of the total available sites, this cell model yields a partition function having the form

$$Z = g(N,y)[v_f(V,y)]^{cN} \exp[-E_0(V,y)/kT] \qquad (1)$$

where g represents the combinatory factor arising from the mixing of molecules and unoccupied sites, v_f is the cell theory free volume function per each three of the total number of $3c$ external degrees of freedom attributed to the chain, and E_0 is the potential energy of the chain with all systems placed in their rest positions.

For molecules and holes placed on a lattice, the volume-dependent part of g is given by

$$g(N,y) \propto y^{-N}(1-y)^{-Ns(1-y)/y} \qquad (2)$$

The free volume internal to the occupied sites v_f, obtained by averaging linearly over single modes of motion, equals

$$v_f/v^* = [y(\tilde{\omega}^{1/3} - 2^{-1/6}) + (1-y)\tilde{\omega}^{1/3}]^3 \qquad (3)$$

where v^* is the characteristic volume per segment (V^*/Ns), $\tilde{\omega}$ is the reduced segmental cell volume, equal to $yV/v^*Ns = yv/v^*$, V is the measured volume of the N molecules, and V^* is the corresponding characteristic scaling volume. The potential energy of the system, assuming a Lennard-Jones interaction between nonbonded segments, is given by

$$2E_0 = yNqx\epsilon^*[1.011\tilde{\omega}^{-4} - 2.409\tilde{\omega}^{-2}] \qquad (4)$$

where qx is the number of nearest-neighbor sites per chain, equal to $s(x-2)+2$, with x the coordination number, and ϵ^* is the characteristic attraction energy per segment.

The Helmholtz free energy is related to the partition function Z by

$$F = -kT \ln Z \qquad (5)$$

From $p = -(\partial F/\partial V)_T$ with $(\partial F/\partial y)_{V,T} = 0$, a reduced equation of state can be written as

$$\tilde{p}\tilde{V}/\tilde{T} = [1 - y(2^{1/2}y\tilde{V})^{-1/3}]^{-1} + (y/\tilde{T})[2.022(y\tilde{V})^{-4} - 2.409(y\tilde{V})^{-2}] \qquad (6)$$

The reduced variables and the characteristic scaling parameters p^*, V^*, and T^* are defined by

$$\begin{aligned} \tilde{p} &= p/p^* = psv^*/(qx\epsilon^*) \\ \tilde{V} &= V/V^* = V/(Nsv^*) \qquad (7) \\ \tilde{T} &= T/T^* = ckT/(qx\epsilon^*) \end{aligned}$$

The subsidiary condition for fixing the fractional occupancy y derived by minimizing the Helmholtz free energy is

$$\begin{aligned} (s/3c)[(s-1)/s + y^{-1}\ln(1-y)] = {}& [y(2^{1/2}y\tilde{V})^{-1/3} - 1/3]/[1 - y(2^{1/2}y\tilde{V})^{-1/3}] + \\ & (y/6\tilde{T})[2.409(y\tilde{V})^{-2} - 3.033(y\tilde{V})^{-4}] \qquad (8) \end{aligned}$$

The characteristic values p^*, V^*, and T^* are obtainable by fitting eq 6 and 8 to experimental data for polymer liquids and are available for a large number of systems.[16]

The relaxation of the glass, involving the rearrangement of molecular segments, is expected to depend on the hole fraction as well as the tendency for the holes to congregate. The latter can be expressed by the local fluctuation in hole fraction. In the following, fractional free volume f will refer to the hole fraction, and not to the cell theory free volume function v_f, which is not expected to play a strong role in segmental diffusion. Therefore, we make the identification

$$f = 1 - y \qquad (9)$$

For a polymer liquid in equilibrium at a given temperature and pressure, eq 6 and 8 yield the reduced volume and occupied fraction y (and unoccupied fraction f) for any pressure and temperature. When the liquid is frozen in the glass in some state away from equilibrium, eq 8 can no longer be used and eq 6 is no longer strictly correct either. However, Simha et al.[17] have shown at least for poly(vinyl acetate) that an adequate approximation to the equation of state could be obtained by using eq 6 with the measured volume V under the actual conditions of p and T. The use of eq 6 along with the measured volume has yielded satisfactory results when applied to time-dependent processes in the glass as well.[13,14,18]

The mean square fluctuations in hole fraction or free volume f can be obtained from eq 1–5. Tolman[19] has shown that the mean square fluctuation in any quantity u about a mean value u_0 is given for small fluctuations by

$$\overline{(u-u_0)^2} = kT/(\partial^2F/\partial u^2)_{u=u_0} \qquad (10)$$

The fluctuation in the free volume f then equals

$$\overline{\delta f^2} = kT/(\partial^2 F/\partial y^2) \qquad (11)$$

where $\delta f = f - \bar{f}$, and $\bar{f}$ is the average free volume. From eq 5 and 1 there follows for a specified V and T

$$\begin{aligned} \left(\frac{\partial^2 F}{\partial y^2}\right)_{V,T} &= kT\left[\frac{1}{Z^2}\left(\frac{\partial Z}{\partial y}\right)_{V,T}^2 - \frac{1}{Z}\left(\frac{\partial^2 Z}{\partial y^2}\right)_{V,T}\right] = \\ & kT\left\{\left(\frac{1}{g}\frac{\partial g}{\partial y}\right)^2 - \frac{1}{g}\frac{\partial^2 g}{\partial y^2} + cN\left[\left(\frac{1}{v_f}\frac{\partial v_f}{\partial y}\right)^2 - \frac{1}{v_f}\frac{\partial^2 v_f}{\partial y^2}\right] + \frac{1}{kT}\frac{\partial^2 E_0}{\partial y^2}\right\} \qquad (12) \end{aligned}$$

From eq 2–4

$$\begin{aligned} \left(\frac{\partial^2 F}{\partial y^2}\right)_{V,T} = kT\Bigg\{ & N_s[1 - 1/s + (2/y)\ln(1-y) + 1/(1-y)]/y^2 + \\ & cN\left[\frac{(2^{1/2}y\tilde{V})^{2/3} - (8/3)y(2^{1/2}y\tilde{V})^{1/3} + 3y^2}{y^2[(2^{1/2}y\tilde{V})^{1/3} - y]^2}\right] + \\ & \frac{Ngx\epsilon^*}{ykT}[6.066(y\tilde{V})^{-4} - 2.409(y\tilde{V})^{-2}]\Bigg\} \qquad (13) \end{aligned}$$

Dividing each term in eq 13 by Ns, the total number of segments, letting $1/s$ approach zero, writing T^* for $qx\epsilon^*/ck$, and setting $s/3c = 1$,[12] we obtain

$$\begin{aligned} Ns\overline{\delta f^2} = \Bigg\{ & [1 + (2/y)\ln(1-y) + 1/(1-y)]/y^2 + \\ & \frac{1}{3}\,\frac{(2^{1/2}y\tilde{V})^{2/3} - (8/3)y(2^{1/2}y\tilde{V})^{1/3} + 3y^2}{y^2[(2^{1/2}y\tilde{V})^{1/3} - y]^2} + \\ & (1/3y\tilde{T})[6.066(y\tilde{V})^{-4} - 2.409(y\tilde{V})^{-2}]\Bigg\}^{-1} \qquad (14) \end{aligned}$$

Because the right-hand side of eq 14 is independent of both N and s, the values for N and s are completely arbitrary, and we may replace the product Ns on the left-hand side by N_s, the number of segments in any size volume in which the fluctuations are desired. Equation 14 expresses the fact that the mean square fluctuations in free volume in particular size volumes times that volume size, as expressed by Ns or N_s, is a constant independent of the volume size. For a polymer liquid in equilibrium, the mean square fluctuation in free volume at any given pressure and temperature is obtained from eq 14 by using values for V and y from eq 6 and 8. When the liquid is frozen in the glass in some state away from equilibrium, eq 14 is used with the measured volume and eq 6.

Kinetics of Volume Change. The changes in volume occurring in the glass during relaxation at constant temperature will be assumed to arise from changes in the hole fraction or free volume. The translation from free volume change to volume change will be made via eq 6. The free volume is assumed to be distributed throughout the entire polymer system, with a variation from region to region that at equilibrium is expressed by the mean square fluctuation in free volume. The rate of change in free volume in a local region is assumed to be a function of the free volume present in that region. Because of the variation in free volume from region to region, the kinetics of free volume change are expected to vary, then, from region to region.

As was done previously,[9,11] it is convenient to treat the free volume in a given region as a discrete variable. Besides being consistent with the cell model, this simplifies the calculation. The distribution of free volume at equilibrium in regions containing N_s segments will be approximated by a binomial distribution for which the mean and the mean square variation from region to region are equal to the global mean free volume and the mean square fluctuation in free volume, respectively. The free volume fraction in any N_s-segment region chosen at random is assigned one of the values 0, β, 2β, ..., $n\beta$, and the free volume unit β and the binomial distribution parameter p are fixed by the mean and the variance of the distribution:

$$np\beta = \bar{f}$$
$$np(1-p)\beta^2 = \overline{\delta f^2} \qquad (15)$$

The $n + 1$ free volume fractions that a N_s-segment region might contain can be treated as $n + 1$ states of the region. The state occupancies at equilibrium given by the binomial distributions are

$$\xi_i = \binom{n}{i} p^i (1-p)^{n-i} \qquad (16)$$

When the system is not necessarily in equilibrium, $w_i(t_0)$ will be used to denote the probability that a region chosen at random at time t_0 is in the ith state; i.e., it contains a fractional free volume equal to $i\beta$. The probability that a region known to be in the ith state at time t_0 has made a transition to the jth state at time t will be denoted by $P_{ij}(t - t_0)$. Because a given region could have been in any of the $n + 1$ possible states at a much earlier time, the current probabilities of state occupation are given by

$$w_j(t) = \sum_{i=0}^{n} w_i(t_0) P_{ij}(t - t_0) \qquad (17)$$

The occupation and transition probabilities have the following properties:

$$\sum_{i=0}^{n} w_i(t) = 1$$
$$\sum_{i=0}^{n} P_{ij}(t - t_0) = 1$$
$$\lim_{h \to 0} P_{ij}(h) = \delta_{ij}$$
$$P_{ik}(t + h) = \sum_j P_{ij}(t) P_{jk}(h) \qquad (18)$$

The last equation allows us to write the time derivative of the P_{ij}'s in the matrix form

$$\dot{\mathbf{P}}(t) = \mathbf{P}(t) \cdot \mathbf{A} \qquad (19)$$

where

$$A_{jk} = \lim_{h \to 0} \frac{\mathrm{d}}{\mathrm{d}h} P_{jk}(h) \qquad (20)$$

It is reasonable to assume that a region undergoing a change from state i to state j will pass through all of the intervening states. Then for an infinitestimal time interval h, the transition probabilities become

$$P_{i,i-1}(h) = h\lambda_i^- + 0(h)$$
$$P_{i,i+1}(h) = h\lambda_i^+ + 0(h) \qquad (21)$$
$$P_{ii}(h) = 1 - h(\lambda_i^- + \lambda_i^+) + 0(h)$$

with all other transition probabilities equal to $0(h)$, where $0(h)$ denotes a quantity that approaches zero faster than h. λ_i^+ is the upward transition rate from state i and λ_i^- is the downward rate. At equilibrium, microscopic reversibility requires

$$\xi_i \lambda_i^+ = \xi_{i+1} \lambda_{i+1}^- \qquad (22)$$

The upward and downward transition rates are expected to depend not only on the local free volume for that region but also on the free volume of its neighbors. This is because for any change in free volume in a given region, the free volume would presumably have to be obtained from or passed onto its neighbors. A strict cell or lattice model would require, even, that the free volume would have to travel to or from the surface of the specimen for any net change in free volume. But with a real amorphous polymer, net changes in free volume are probably liberated and adsorbed by changes in various local strains of the system. Moreover, the kinetics of contraction and dilatation of real polymer glasses, instead of suggesting that the free volume must travel between the interior and the surface, indicate that the kinetics are only slightly sensitive, if at all, to the specimen size.[7] At equilibrium there is no correlation between the free volume content of neighboring regions. Assuming that the correlation remains weak away from equilibrium, we can approximate the combined free volume of the neighboring regions by the average free volume of the entire specimen. Hence, we assume that the transition rate for the region of interest out of a state i depends on the free volume $\hat{f}_i$ given by

$$\hat{f}_i = [i\beta + (z-1)\bar{f}]/z \qquad (23)$$

where z is a measure of the number of regions needed to liberate or absorb net free volume changes in the region of interest.

To obain the functional dependence of the local transition rates λ_i^+ and λ_i^- on free volume, we will assume, first, that the local dependence is the same as the global dependence. Equations with the following form have been found to describe fluidity vs. temperature for most polymer and many nonpolymer liquids and to describe the viscoelastic time–temperature shift parameters. Writing the rates of mobility as the reciprocal of a relaxation time, we have

$$\tau^{-1}(T) = \tau_g^{-1} \exp\left\{2.303 c_1 \frac{T - T_g}{c_2 + T - T_g}\right\} \qquad (24)$$

where the subscript g's refer to the glass transition, which is taken as the reference temperature.[20] Following Williams, Landel, and Ferry, we assume next that the temperature dependence shown in eq 24 actually represents the free volume dependence. Instead of the free volume definition used by Williams, Landel, and Ferry, however, we use that defined by eq 6, 8, and 9. Over small intervals of temperature, f is nearly linearly related to the temperature and we can write

$$f - f_g = a_{\text{liq}}(\tilde{T} - \tilde{T}_g) \qquad (25)$$

Hence, the relaxation rate can be written as

$$\tau^{-1}(f) = \tau_g^{-1} \exp\left\{2.303c_1 \frac{f - f_g}{a_{\text{liq}}c_2/T^* + f - f_g}\right\} \qquad (26)$$

We assume finally that the relaxation rate has this local dependence on free volume irrespective of whether or not the global system is in equilibrium. The rates of local changes in state are written, then, as[10]

$$\lambda_i^- = R\tau_g^{-1}(\xi_{i-1}/\xi_i)^{1/2}\beta^{-2} \exp\left\{2.303c_1 \frac{\hat{f}_i - f_g}{a_{\text{liq}}c_2/T^* + \hat{f}_i - f_g}\right\}$$

$$\lambda_i^+ = \lambda_{i+1}^-(\xi_{i+1}/\xi_i) \qquad (27)$$

where the terms in the front factor arise in the following way. R is a numerical constant that adjusts the global kinetics to that locally and compensates numerically for the other terms in the front factor. $(\xi_{i-1}/\xi_i)^{1/2}$ enforces the microscopic reversibility expressed by eq 22 and is written in this way so it enters both the upward and downward rates similarly. β^{-2}, where β is the step between adjacent free volume states, arises from the discrete random walk representation of a continuous diffusion process.

From eq 20 and 21, the matrix elements of **A** become

$$A_{i,i-1} = \lambda_i^-, \qquad i = 1, 2, ..., n$$

$$A_{ii} = -(\lambda_i^- + \lambda_i^+), \qquad i = 0, 1, ..., n$$

$$A_{i,i+1} = \lambda_i^+, \qquad i = 0, 1, ..., n - 1$$

$$A_{ij} = 0, \qquad \text{if } j \neq i - 1, i, i + 1 \qquad (28)$$

Because λ_i^- is not generally equal to λ_{i-1}^+, **A** is not generally a symmetric matrix. But because all of the off-diagonal terms are positive, a similarity transform can be applied to **A** to create a symmetric matrix **Z**:

$$\mathbf{Z} = \gamma^{-1}\mathbf{A}\gamma \qquad (29)$$

Since **A** is tridiagonal, γ need only be diagonal to effect this transformation, and n elements of γ can be obtained from the n equations

$$Z_{i,i-1} = A_{i,i-1}\gamma_{i-1}/\gamma_i = A_{i-1,i}\gamma_i/\gamma_{i-1} = Z_{i-1,i}$$

or

$$\gamma_{i-1}/\gamma_i = (A_{i-1,i}/A_{i,i-1})^{1/2} = (\xi_i/\xi_{i-1})^{1/2} \qquad (30)$$

Since one of the $n + 1$ elements of γ is left undetermined, it may be chosen so that

$$\gamma_i = \xi_i^{-1/2} \qquad (31)$$

The nonzero matrix elements of **Z** are then

$$Z_{i,i-1} = \lambda_i^-(\xi_i/\xi_{i-1})^{1/2}$$

$$Z_{ii} = -(\lambda_i^- + \lambda_i^+) \qquad (32)$$

$$Z_{i,i+1} = \lambda_{i+1}^-(\xi_{i+1}/\xi_i)^{1/2}$$

The differential equation in eq 19 becomes

$$\mathrm{d}(\mathbf{P}\gamma)/\mathrm{d}t = \mathbf{P}\gamma\mathbf{Z} \qquad (33)$$

with the formal solution

$$\mathbf{P}(t) = \mathbf{P}(0)\gamma \exp(\mathbf{Z}t)\gamma^{-1} \qquad (34)$$

Because of the properties of the P's, $\mathbf{P}(0)$ equals the unit matrix. The exponential factor when expressed in its infinite series expansion is readily summed after expressing **Z** in terms of its eigenvectors and eigenvalues to give

$$\mathbf{P}(t) = \gamma\mathbf{QEQ}^{-1}\gamma^{-1} \qquad (35)$$

where **Q** is the matrix formed from the $n + 1$ eigenvectors of **Z**, corresponding to the $n + 1$ eigenvalues ζ, $\mathbf{Q}^{-1}$ equals the transpose of **Q** because **Z** is symmetric, and **E** is a diagonal matrix with the elements $E_k = \exp(\zeta_k t)$. Among the eigenvalues of **Z**, one is zero, corresponding to the steady state, after an infinite length of time, and all the rest are finite and negative.

The probability of state i existing at time t is given by

$$w_i(t) = \sum_{k=0}^{n} \gamma_i^{-1}Q_{ik}[\sum_{j=0}^{n} w_j(t_0)\gamma_j Q_{jk}] \exp[\zeta_k(t - t_0)] \qquad (36)$$

When $t = \infty$, $w_i = \xi_i$. The average free volume in the glass at any instant of time t is given, then, by

$$\bar{f}(t) = \sum_{i=0}^{n} i\beta w_i(t) \qquad (37)$$

As mentioned above, the volume of the polymer may be related to the free volume through eq 6. The effective retardation time for approach to equilibrium can be written as

$$\tau^{-1} = -(\mathrm{d}V/\mathrm{d}t)(V - V_{\text{eq}})^{-1} \doteq -(\mathrm{d}\bar{f}/\mathrm{d}t)(\bar{f} - \bar{f}_{\text{eq}})^{-1} \qquad (38)$$

because V changes nearly linearly with $\bar{f}$. The subscript "eq" refers to equilibrium. Letting ζ_0 be the zero eigenvalue and writing $\bar{f}(t) = \sum C_k \exp(\zeta_k t)$, we have

$$\tau^{-1} \doteq -\sum_{k=1}^{n} \zeta_k C_k \exp(\zeta_k t) / \sum_{k=1}^{n} C_k \exp(\zeta_k t) \qquad (39)$$

The above computation assumes that the transition rates do not change during the course of time. In fact, the transition rates do change with time because the rates depend through eq 27 and 23 on the average free volume. However, the transition rates have been found to change slowly enough with time that no significant error is incurred by allowing the relaxation to evolve according to eq 36 and 37 and only intermittently stopping the process to reevaluate the average free volume. For example, increments of time during which the average free volume changes by an amount equivalent to a temperature change in the liquid of 1 K have been found to be short enough to avoid significant error. Thus, during the relaxation following a temperature step of 10 K, no more than 10 relaxation increments need be made. Greater, through usually unnecessary, accuracy can be obtained by shorter time increments, of course. In the actual computation, t_0 is set equal to the end of the last time increment and t is allowed to increase until the average free volume in eq 37 has changed by an amount corresponding to 1 K, or whatever is desired. At this point the transition rates are recalculated from eq 23 and 27, the matrix **Z** is again diagonalized, and the initial time t_0 and occupation probabilities $w_j(t_0)$ are advanced to the end of the last time increment to start the relaxation process going again.

Results for Poly(vinyl acetate)

The theory will be applied to poly(vinyl acetate), the polymer for which the volume retardation was extensively

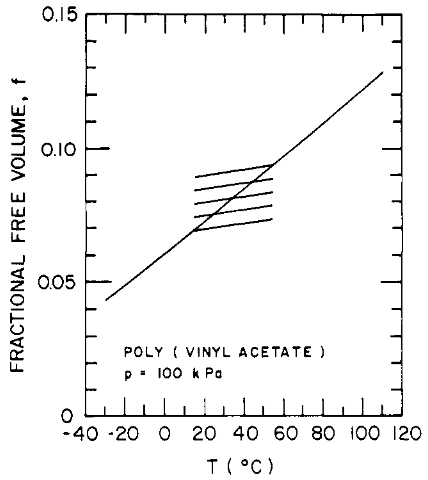

Figure 1. Free volume of poly(vinyl acetate) at 100-kPa pressure computed for the liquid and for five glass states.

studied by Kovacs.[15] The characteristic thermodynamic parameters for poly(vinyl acetate) are[21]

$$p^* = 938.0 \text{ MPa}$$
$$V^* = 814.1 \text{ mm}^3/\text{g} \qquad (40)$$
$$T^* = 9419. \text{ K}$$

The free volume of the equilibrium liquid at 100 kPa (1 bar) pressure computed from eq 6 and 8 is shown in Figure 1 plotted against temperature and extended into the glassy region. Also shown in Figure 1 are five glass curves obtained from eq 6 with

$$V = V_0[1 + \alpha_{\text{glass}}(T - T_0)] \qquad (41)$$

where V_0 and T_0 refer to the liquid at the points where the glass curves intersect the liquid curve. The volume expansivity of 2.4×10^{-4} K^{-1} was adopted for each of the glasses. The different glass curves may be thought of as representing glasses formed at different cooling rates. Their actual origin and use are described below. The mean square fluctuation in free volume of the equilibrium liquid at 100-kPa pressure obtained from eq 6, 8, and 14 is shown plotted against temperature in Figure 2. Also shown are glass curves corresponding to those in Figure 1 obtained from eq 6, 41, and 14. The glass curves are seen to be much more parallel to the liquid curve for the mean square fluctuation than for the free volume itself.

An experiment of great importance in illustrating the physical aging of plastics has been the single-temperature-step experiment. In this experiment, a polymer specimen at equilibrium at temperature T_0 is rapidly heated or cooled to the temperature T_l, and then the physical aging or relaxation of the specimen toward equilibrium at T_l is followed. To simulate these experiments analytically, we will assume an instantaneous change in temperature from T_0 to T_l. From given positions on the liquid curves in Figures 1 and 2, the specimen's free volume and mean square fluctuation in free volume are assumed to shift along or parallel to the glass curves with the instantaneous change in temperature. The relaxation process, occurring at constant temperature, then follows vertical lines from the appropriate glass curves toward the liquid curves in Figures 1 and 2.

To begin the calculation of the relaxation kinetics, a value for N_s is required. From previous considerations of allowable molecular motion,[8] a minimum of 26 monomer units was estimated to be involved in any motion. This estimate assumed a single pair of monomer units undergoing a rearrangement in the environment of 12 neighboring pairs. N_s will be set equal to 26 in the calculation described below, but it may refer to more than 26 monomer units. N_s refers to molecular segments with three degress of allowable motion. The motion sustained by the single pair of monomers mentioned above involved from three to five bonds changing conformation simultaneously. At least in the liquid state, actual reaction kinetics and computer-simulated reaction kinetics suggest that no more than one bond changes conformation at a time.[22,23] The interpretation of this is that to accommodate a large change in rotational angle by a single bond, several adjacent bonds along the chain must make incremental changes in rotational angle. The inclusion of these neighboring monomers could double or triple the number of monomers. The volume occupied at 35 °C and 100 kPa by 26 monomers by poly(vinyl acetate) is 3.2 nm^3, which is that of a 1.8-nm-diameter sphere.

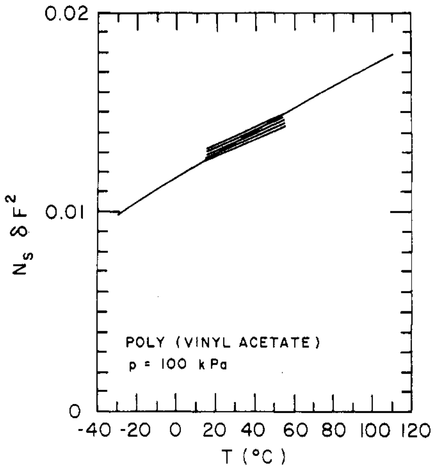

Figure 2. Mean square fluctuation in free volume times the number of segments filling the region of interest of poly(vinyl acetate) at 100-kPa pressure computed for the liquid and five glass states.

The glass obtained immediately after shifting the temperature to T_l from T_0, where the substance had been in equilibrum, will be assumed to have its free volume distributed according to a binomial distribution. The parameters for this distribution are obtained from eq 15 after obtaining values for $\bar{f}$ and $\overline{\delta f^2}$ from eq 6, 41, and 14 for the glass at the temperature T_l and choosing a value for n. The free volume of the equilibrium liquid at T_l is assumed also to be distributed according to a binomial distribution, and to be able to keep β constant throughout the relaxation process, a different value for n may need to be chosen for the equilibrium liquid. Equations 15 yield

$$n_l = \bar{f}_l/(\beta - \overline{\delta f_l^2}/\bar{f}_l) \qquad (42)$$

where the subscript l refers to the equilibrium liquid at temperature T_l. The value of n_l needed is the value from eq 42 rounded off to the nearest integer. To avoid an inconsistency from the rounding, the binomial distribution parameter p is chosen so that $\bar{f}_l$ is exact and $\overline{\delta f_l^2}$ is approximated by $\bar{f}_l(\beta - \bar{f}_l/n_l)$.

The values of various other parameters used in the calculation of the relaxation kinetics are given in Table I. z was equated to 13 to represent the N_s-segment region of interest and its 12 nearest neighbors, assuming a coordination on the faces of a dodecahedron. n was usually chosen as 15, which was found to leave n_l at n and to minimize the error in $\overline{\delta f_l^2}$ for steps between temperatures in the vicinity of the glass transition for poly(vinyl acetate). a_{liq} was computed for each simulated experiment from eq 25; T_l and f_l were used for T and f except when they

Table I
Calculation Parameters for the Relaxation Kinetics

$N_s = 26$	no. of segments in free volume region
$c_1 = 15.6^a$ $c_2 = 46.8\ K^a$	time-temperature shift parameters
$T_g = 308.$ K	glass transition at 100 kPa
$f_g = 0.08134$	free volume at glass transition and 100 kPa
$\tau_g = 1$ h (3600 s)	relaxation time at glass transition
$z = 13$	size ratio for region controlling free volume

[a] Ferry, J. D. "Viscoelastic Properties of Polymers", 2nd ed.; Wiley: New York, 1970; p 316.

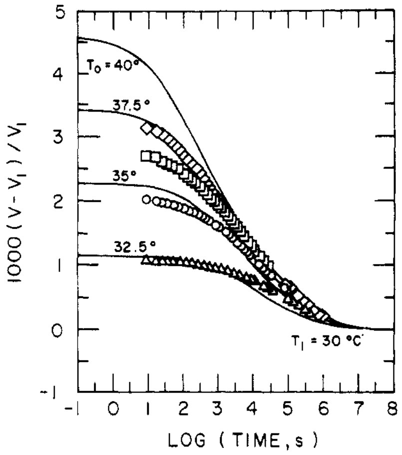

Figure 3. Computed curves and experimental data on the relative deviation of the volume from equilibrium vs. log (time) following steps in temperature to 30 °C from 40 (◇), 37.5 (□), 35 (○), and 32.5 °C (△) for poly(vinyl acetate). Data from Kovacs.[15]

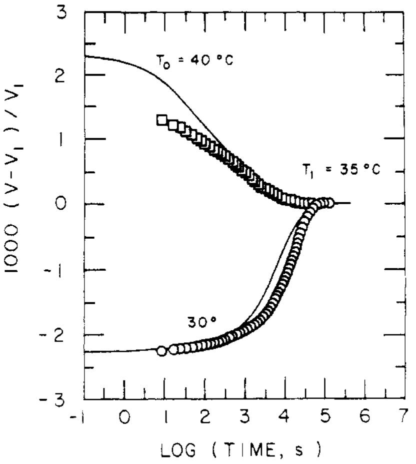

Figure 4. Computed curves and experimental data on the relative deviation of the volume from equilibrium vs. log (time) following steps in temperature to 35 °C from 40 (□) and 30 °C (○) for poly(vinyl acetate). Data from Kovacs.[15]

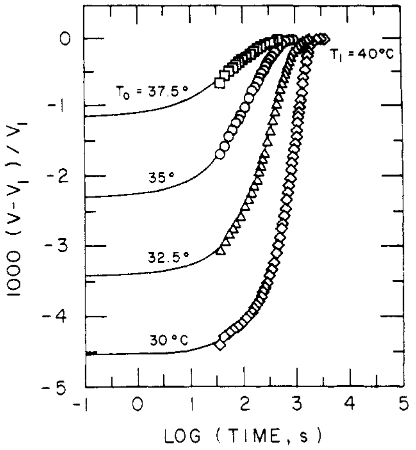

Figure 5. Computed curves and experimental data on the relative deviation of the volume from equilibrium vs. log (time) following steps in temperature to 40 °C from 30 (◇), 32.5 (△), 35 (○), and 37.5 °C (□) for poly(vinyl acetate). Data from Kovacs.[15]

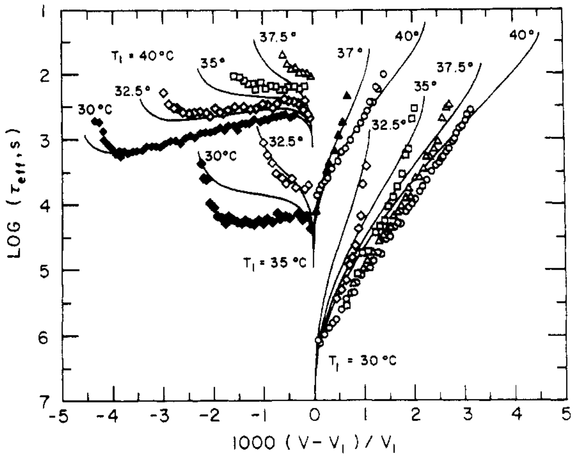

Figure 6. Computed curves and experimental data on the effective retardation times for temperature-step experiments for poly(vinyl acetate) at 100 kPa. The group of curves on the left are for upsteps in temperature to 35 and 40 °C, respectively; those on the right are for downsteps to 30 and 35 °C, respectively. The assumed glass temperature was 35 °C. Data from Kovacs.[15]

equaled T_g and f_g, in which case infinitesimal deviations from T_g and f_g were used.

The computed approach to equilibrium is compared in Figures 3–5 with the experimental data of Kovacs on poly(vinyl acetate) at 100-kPa pressure.[15] The computed curves in Figure 3 are for four simulated experiments in which the polymer had been in equilibrium at 40, 37.5, 35, and 32.5 °C, respectively, and were instantaneously stepped to 30 °C. The data correspond to the same experiments except the temperature was changed over times of the order of a minute. The computed curves and data in Figure 4 refer to the steps in temperature to 35 °C from equilibrium at 40 and 30 °C, respectively. And the computed curves and data in Figure 5 refer to the steps in temperature to 40 °C from equilibrium at 30, 32.5, 35, and 37.5 °C, respectively.

The computed effective retardation times vs. the deviation of the volume from equilibrium are compared with those derived from experiment in Figure 6. The groups of curves on the left in Figure 6 are for upsteps in temperature to 40 and 35 °C, respectively, and those on the right for downsteps to 35 and 30 °C, respectively. The comparison of the effective retardation times vs. deviation of the volume from equilibrium in Figure 6 is somewhat more critical than is the comparison of the recovery curves of volume vs. log (time) in Figures 3–5.

The computed curves in Figures 3–6 have been shifted as a group along the time axes to produce the best fit to the data and thereby determine the value for the unknown parameter R in eq 27. The computed curves in Figure 6, though shifted as a group to yield an overall fit, were shifted to give the best fit to the data for the upstep from 30 to 40 °C. The resulting value of R was 7.3×10^{-4}. The best overall fit of the computed curves to the data in Figures 3 and 5 resulted in values of R of 15.6×10^{-4} and 5.8×10^{-4}, respectively. These different values of R at 30 and 40 °C, respectively, suggested for R the form R_0 exp-$[H^{\ddagger}kT]$, with $H^{\ddagger} = 78$ kJ/mol. The computed curves in Figure 4 were shifted with the same values for R_0 and $H^{\ddagger}$ that best fitted Figures 3 and 5.

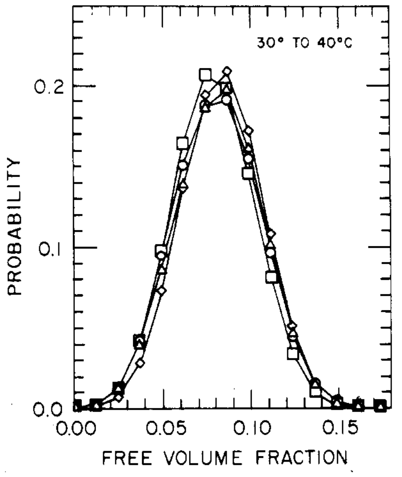

Figure 7. Computed distribution of free volume among 26-segment regions in poly(vinyl acetate) at 100-kPa pressure for the step from 30 to 40 °C, initially (□), finally at equilibrium (◇), and at two intermediate times (○ and △).

In general, the fit between the computed curves and the data is fairly good. The best fit was obtained for the four upstep experiments to 40 °C in Figure 5. The poorest fit is probably for the upstep from 30 to 35 °C in Figure 4 and again in Figure 6. The downstep experiments in Figures 3 and 4 are not well fitted at early times, but this is due to the gradual, rather than an instantaneous, temperature change in the experiment. The gradual temperature change affects the fit for downward temperature changes more than for upward temperature changes because the cooler initial temperature in the latter delays the volume change until the new, higher temperature is nearly attained. In contrast, so much relaxation occurs before the new temperature is attained in the downward step that the wrong initial volumes would be deduced from extrapolating these data backward in time.

The feature of Kovacs' data in Figure 6 that has been the most difficult to explain has been the apparent lack of convergence of the retardation curves from an upstep in temperature as equilibrium is approached. The computed curves seem eventually to converge at equilibrium, but the convergence begins to occur in only the last few percent of deviation from equilibrium. The delayed convergence arises from the way in which the free volume distribution changes in response to a temperature step. Figure 7 shows the probability distribution for the fractional free volume content of groups of 26 segments at four times during the upward step from 30 to 40 °C: the initial distribution (denoted by squares), the final equilibrium distribution (denoted by diamonds), and two intermediate distributions. The upper end of the distribution equilibrates soon after the temperature step, but the lower end of the distribution equilibrates only near the end of the retardation process. Moreover, the kinetics of the process continues to be affected by the low free volume tail of the distribution, depending on the degree to which the initial and final low free volume tails differ, until equilibrium is reached. As a result, the volume dilatation resulting from the upstep in temperature from 37.5 to 40 °C appears in Figure 5 to reach equilibrium long before the upstep from 30 to 40 °C, for example. On the other hand, because the initial and final low free volume tails of the two experiments represented in Figure 4 are predicted to differ by the same amount because each is a 5 °C step, though the sign of the free volume change in the tail is opposite, the two experiments are expected to reach equilibrium at the same time. But the data indicate that the downstepped experiment is faster.

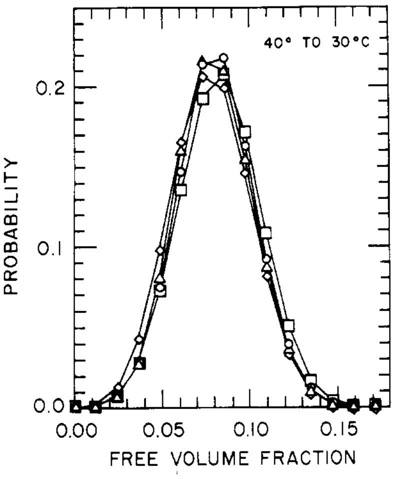

Figure 8. Computed distribution of free volume among 26-segment regions in poly(vinyl acetate) at 100-kPa pressure for the step from 40 to 30 °C, initially (□), finally at equilibrium (◇), and at two intermediate times (○ and △).

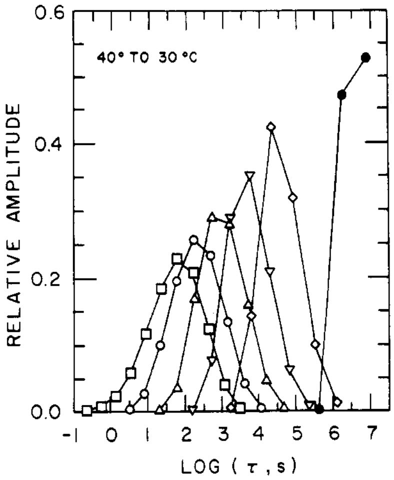

Figure 9. Retardation time spectra at stages during the volume recovery following the temperature step from 40 to 30 °C. Progression from the initial spectrum (□), immediately after the step, to the final spectrum (●).

The changes in the free volume distribution for the downstep experiment from 40 to 30 °C are shown in Figure 8. As in Figure 7, the initial distribution (denoted by squares), the final distribution (denoted by diamonds), and two intermediate distributions are shown. As before, the low free volume end of the distribution adjusts to the temperature step only just before equilibrium is reached. More dependence on the initial temperature is predicted for the downstepped experiments in Figure 3 than seems to be indicated by the data.

The computed retardation time spectra for two experiments, a downstep from 40 to 30 °C and an upstep from 30 to 40 °C, are shown in Figure 9 and 10. The different curves in each figure are the retardation spectra at different times during the relaxation process, progressing from the initial spectrum following the instantaneous jump in temperature (denoted by squares) to the final spectrum just as equilibrium is being reached (denoted by filled circles). The spectra are actually discrete but are here shown with the tips of the spectral lines joined together for clarity. Each spectral line is weighted according to the remaining deviation from equilibrium of the free volume state giving rise to the line. Because the lines were normalized for height and not for area under the curve, the area under these curves increases as the relaxation progresses because the significant spectra lines become fewer

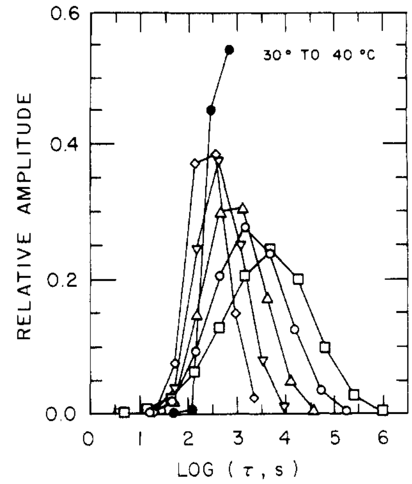

Figure 10. Retardation time spectra at stages during the volume recovery following the temperature step from 30 to 40 °C. Progression from the initial spectrum (□), immediately after the step, to the final spectrum (●).

and therefore gain in relative importance. In the downstep experiment, the spectrum is seen to move monotonically to longer times, consistently with the corresponding effective retardation times in Figure 6. The left-hand or short-time side of the spectrum moves to longer times slightly faster than does the right-hand side. The result is that the spectrum tends to narrow. In the upstep experiment the center of the spectrum is seen to move generally toward shorter times and the back toward longer times at the end, as occurs with the corresponding retardation times in Figure 6. Through most of the relaxation, the right-hand or longer retardation time side of the spectrum moves toward shorter times while the left-hand side remains relatively stationary. A changing retardation spectrum during the relaxation process has also been suggested by Matsuoka.[24]

Discussion

Overall, the current model, using free volume from Simha's equation of state and fluctuations in free volume derived from Simha's partition function with the stochastic model used by Robertson, successfully describes the volume retardation data of Kovacs on poly(vinyl acetate). In particular, the model is generally able to deal with different apparent arrival times at equilibrium for specimens coming from different temperatures. The only exception is the different apparent arrival times at equilibrium at 35 °C from 30 and 40 °C. The reason for the greater success in the present computation than previously[11] is due to the use of more free volume states (16 vs. 8 previously) and to the use of a free volume function that results in a larger average free volume (0.081 at the glass transition temperature vs. 0.025). As mentioned, the history dependence results from the low free volume tail of the distribution, and both the larger number of states and the larger average free volume allow greater resolution of this part of the free volume distribution.

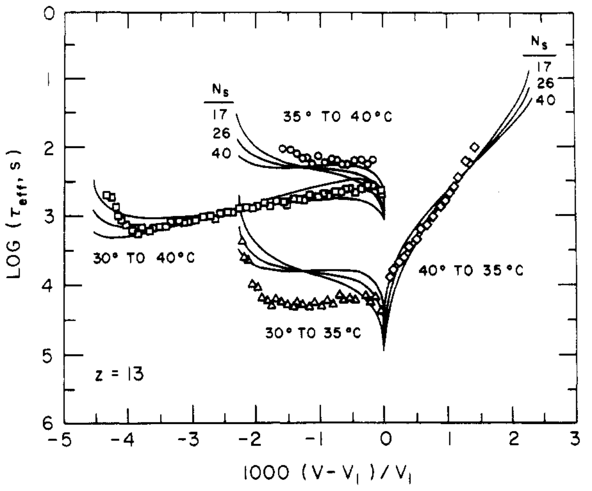

Figure 11. Effective retardation times vs. relative deviation of the volume from equilibrium computed with three different values for N_s, 17, 26, and 40 ($z = 13$), for four different temperature-step experiments: the upsteps from 30 and 35 °C to 40 °C, the upstep from 30 to 35 °C, and the downstep from 40 to 35 °C. Data from Kovacs.[15]

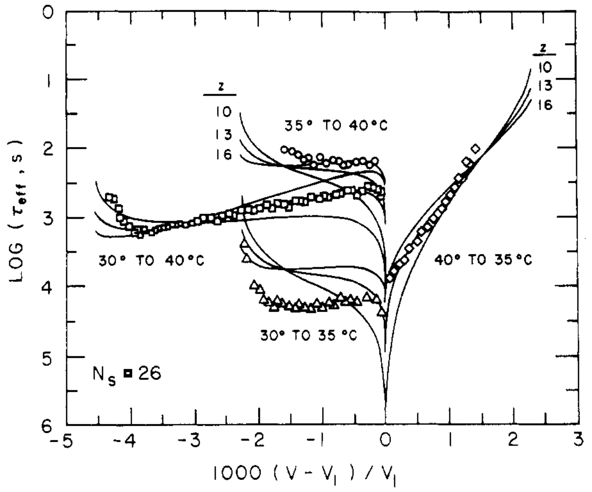

Figure 12. Effective retardation times vs. relative deviation of the volume from equilibrium computed with three different values for z, 10, 13, and 16 ($N_s = 26$), for four different temperature-step experiments: the upsteps from 30 and 35 °C to 40 °C, the upstep from 30 to 35 °C, and the downstep from 40 to 35 °C. Data from Kovacs.[15]

The model makes use of a number of parameters. The main adjustable parameter is R, which shifts the computed curves along the time or effective retardation time axis without changing their shape. Although R was given an Arrhenius form in fitting the data in Figures 3–5, R should be only weakly dependent on temperature, perhaps proportional to kT, theoretically. The Arrhenius form was used to compensate for the deviation between the actual viscoelastic behavior of the poly(vinyl acetate) specimens in the temperature region studied by Kovacs and that described by the WLF equation with the c's given in Table I. N_s and z are two other adjustable parameters, though their values are constrained by their physical meaning. The effect that N_s and z have on the computed effective retardation times is shown in Figures 11 and 12, respectively. (R was held fixed at 7.3×10^{-4} for each of these curves.) N_s and z are seen to have similar effects, though the curves are somewhat more sensitive to changes in z than to changes in N_s. N_s and z cause the curves to rotate about a fixed point a certain fractional distance between the initial and equilibrium states. The reason that N_s and z have an analogous effect on the computed curves is seen by combining eq 14 and 15 with eq 23. Denoting the right-hand side of eq 14 by $h(p,V,T)$, we have

$$\hat{f}_i = \frac{ih(p,V,T)}{zN_s\bar{f}} + \bar{f}\left[1 - \frac{n-i}{nz}\right] \qquad (43)$$

z appears by itself in the second term but appears as a product with N_s in the first term. N_s appears only in this product. For free volume states i near n, states that dominate the early relaxation, the dependence on z in the second term is minimal, and it is only the product with

N_s that is significant. But for free volume states of small i, states that dominate the relaxation behavior near equilibrium, the z dependence in the second term becomes more important. This is seen in comparing Figures 11 and 12. Although the values of N_s and z remained constant in all the curves shown in Figures 3–10, it is possible that their values should have been allowed to change during the relaxation process and for different step temperatures.

Two other parameters were varied while applying the model. These were the number of free volume states and the number of iterative steps taken during the structural recovery. The iterative steps are needed to allow for the changing free volume, as mentioned earlier. Neither parameter affects the general predictions of the model, but they do affect the continuity of the curves. For the curves in Figures 3–6, 11 and 12, the number of iterative steps was 4 per degree of temperature. Thus, for example, 20 iterative steps were taken for the 5 °C temperature step from 30 to 35 °C. Also, an additional step was taken near the beginning and two near the end of the process to obtain more continuity in the curves. Although it would not have been necessary to reevaluate the average free volume more often than every 1 °C of change in equivalent temperature, as was mentioned earlier, it was easily done as the state of the system was evaluated at each of these times. As mentioned earlier, the number of free volume states assumed was 16 because this was found to minimize the error in the assumed free volume fluctuation for the final state.

The current approach is successful also as a computational procedure. Much of the computational time needed is used in finding the eigenvalues and eigenfunctions of 16 × 16 symmetrical, tridiagonal matrices, for which a program from EISPACK was used. Approximately 0.4 s of CPU time on a time-sharing DEC-20 was needed for this plus associated element summings. Thus, for example, with 24 diagonalizations performed, one for each of the iterative steps plus one for the initial state, the computation of the relaxation process for the 5 °C upstep from 30 to 40 °C required only 10 s of CPU time.

The nature of the approximation in using the mean fluctuations in free volume given by eq 14 should be mentioned. First, it is implicitly assumed in using eq 10 for mean square fluctuations that the first derivative, $(\partial F/\partial y)_{V,T}$, is zero. When the system is described by the partition function in eq 1, this will not be true generally for the glass. One could assume that the forces that retain the polymer in a particular glassy state can be approximated by an additional, albeit weakly time-dependent, term in the partition function that yields a zero first derivative of the free energy but which does not affect strongly the second derivative. In fact, our use of eq 14 is consistent with this assumption. The only use made of eq 14 in the glass is to evaluate the shift in the magnitude of the fluctuations as the temperature is instantaneously changed away from a temperature where the system had been in equilibrium; it is not used to compute the dynamic fluctuations in free volume. The number of empty lattice sites or cells that constitutes the free volume in Simha and Somcysky's model seems to depend on the effective size of the segment, which probably depends on both the flexibility of the chain and the size of the deformed segment in Brownian impact. One result is that the free volume increases with increasing temperature faster than does the volume. In addition, the free volume is dependent on temperature even without molecular rearrangement, and this is probably the principal source of free volume change in the glass as the temperature is changed. Because of the intrinsic dependence of free volume on temperature, equations like eq 6, 41, and 14 are needed to compute the instantaneous change in the mean free volume and fluctuations about the mean. As numerical approximations, eq 6, 41, 14 are certainly adequate for small jumps in temperature, where the system is not far removed from equilibrium. With large jumps in temperature, however, some error may arise.

Second, fluctuations about the mean are generally assumed to be small compared with the magnitude of that mean. But from the free volume distribution shown in figures 7 and 8, the free volume fluctuations appear to be fairly large compared with the mean. However, the statistical mechanical calculation refers to the number of occupied cells rather than the unoccupied cells as shown here. That is, the fluctuation in free volume, which equals the fluctuation in the number of occupied cells, needs to be compared with the mean number of occupied cells. On this basis, the fluctuations seem much smaller. Hence, the error in assuming that the free volume fluctuations are small compared with the mean is probably no larger than that from the use of a discrete binomial distribution for free volume.

Note Added in Proof: We have just found that the separate shifting of the groups of curves for T_1 = 30, 35, and 40 °C is obviated by using the time–temperature shift parameters recently reported [Plazek, D. J. *Polym. J.* **1980**, *12*, 43] for poly(vinyl acetate) in the "softening region".

Registry No. Poly(vinyl acetate), 9003-20-7.

References and Notes

(1) Chow, T. S.; Prest, W. M. *J. Appl. Phys.* **1982**, *53*, 6568.

(2) Kovacs, A. J.; Hutchinson, J. M.; Aklonis, J. J. In "The Structure of Non-Crystalline Materials", Gaskell, P. H., Ed.; Taylor and Francis: London, 1977; pp 153–163.

(3) Kovacs, A. J.; Aklonis, J. J.; Hutchinson, J. M.; Ramos, A. R. *J. Polym. Sci., Polym. Phys. Ed.* **1979**, *17*, 1097. Kovacs, A. J. *Ann. N.Y. Acad. Sci.* **1981**, *371*, 38.

(4) Debolt, M. A.; Easteal, A. J.; Macedo, P. B.; Moynihan, C. T. *J. Am. Ceram. Soc.* **1976**, *54*, 491.

(5) Moynihan, C. T.; Macedo, P. B.; Montrose, C. J.; Gupta, P. K.; Debolt, M. A.; Dill, J. F.; Dom, B. E.; Drake, P. W.; Easteal, A. J.; Elterman, P. B.; Moeller, R. P.; Sasabe, H.; Wilder, J. A. *Ann. N.Y. Acad. Sci.* **1976**, *279*, 15.

(6) Hodge, I. M.; Berens, A. R. *Macromolecules* **1982**, *15*, 762.

(7) Curro, J. G.; Lagasse, R. R.; Simha, R. *Macromolecules* **1982**, *15*, 1621.

(8) Robertson, R. E. *J. Polym. Sci., Polym. Symp.* **1978**, *No. 63*, 173.

(9) Robertson, R. E. *J. Polym. Sci., Polym. Phys. Ed.* **1979**, *17*, 597.

(10) Robertson, R. E. *J. Appl. Phys.* **1978**, *49*, 5048.

(11) Robertson, R. E. *Ann. N.Y. Acad. Sci.* **1981**, *371*, 21.

(12) Simha, R.; Somcynsky, T. *Macromolecules* **1969**, *2*, 342.

(13) Curro, J. G.; Lagasse, R. R.; Simha, R. *J. Appl. Phys.* **1981**, *52*, 5892.

(14) Lagasse, R. R.; Curro, J. G. *Macromolecules* **1982**, *15*, 1559.

(15) Kovacs, A. J. *Fortsch. Hochpolym. Forsch.* **1963**, *3*, 394.

(16) Olabisi, O.; Simha, R. *Macromolecules* **1975**, *8*, 211. Zoller, P. *J. Polym. Sci., Polym. Phys. Ed.* **1978**, *16*, 1491.

(17) McKinney, J. E.; Simha, R. *Macromolecules* **1976**, *9*, 430 and references to previous papers therein.

(18) Jain, S. C.; Simha, R. *Macromolecules* **1982**, *15*, 1522.

(19) Tolman, R. C. "The Principles of Statistical Mechanics"; Oxford University Press: New York, 1938; p 640.

(20) Williams, M. L.; Landel, R. F.; Ferry, J. D. *J. Am. Chem. Soc.* **1955**, *77*, 3701.

(21) McKinney, J. E.; Simha, R. *Macromolecules* **1974**, *7*, 894.

(22) Morawetz, H. *Science (Washington, D.C.)* **1979**, *203*, 405.

(23) Helfand, E.; Wasserman, Z. R.; Weber, T. A. *Macromolecules* **1980**, *13*, 526.

(24) Matsuoka, S., private communication, 1983.